

# Geometric Representation of Fundamental Particles' Inertial Mass

L. Schächter<sup>1</sup> and J. Spencer<sup>2</sup>

<sup>1</sup>*Technion-Israel Institute of Technology, Haifa 32000, Israel*

<sup>2</sup>*SLAC National Accelerator Laboratory, Menlo Park, CA 94025-7015, USA*

(Dated: July 22, 2015)

A geometric representation of the ( $N = 279$ ) masses of quarks, leptons, hadrons and gauge bosons was introduced by employing a Riemann Sphere facilitating the interpretation of the  $N$  masses in terms of a single particle, the Masson, which might be in one of the  $N$  eigen-states. Geometrically, its mass is the radius of the Riemann Sphere. Dynamically, its derived mass is near the mass of the nucleon regardless of whether it is determined from all  $N$  particles or only the hadrons, the mesons or the baryons separately. Ignoring all the other properties of these particles, it is shown that the eigen-values, the polar representation  $\theta_\nu$  of the masses on the Sphere, satisfy the symmetry  $\theta_\nu + \theta_{N+1-\nu} = \pi$  within less than 1% relative error. These pair correlations include the pairs  $\theta_\gamma + \theta_{\text{top}} \simeq \pi$  and  $\theta_{\text{gluon}} + \theta_{\text{H}} \simeq \pi$  as well as pairing the weak gauge bosons with the three neutrinos. The eigen-values form 6 distinct clusters. A function was established whose zeros were a good approximation to the masses  $\{\theta_\nu\}$ . It was shown that there are very few particles with spin ( $J$ ) larger than  $1 + \theta^3$  and no particles having  $\theta > 0.6\pi$  with a spin larger than 2.

## I. INTRODUCTION

Mass is a property of matter that we take for granted but, other than experimental data, little is known about its origins or composition. At the macroscopic level it was first taken by Newton to summarize all the irreducible properties of a body<sup>1</sup> and especially inertia or the resistance to motion. Further, because force per se was invisible while mass manifests itself in all observable bodies, it was mass that defined force for Newton and not the reverse. Later Einstein<sup>2</sup> postulated that the gravitational mass equaled the inertial mass that might include energy in various forms some of which appeared to have no ponderable mass whatsoever.

At the microscopic level, it is taken first as a parameter in a Hamiltonian and after renormalization the resultant value is taken to be the inertial mass of a particle.<sup>3</sup> We take these values as given.<sup>4,5</sup> At the low-energy end we find a degenerate pair of zero mass bosons (the photon and gluon) and the three neutrinos (electron, muon and tau).<sup>6</sup> At the high-energy end are the gauge bosons  $W^\pm$  and  $Z$ , the Higgs and the top quark.

Spanning from zero to more than 100GeV, we introduce a geometric representation allowing us to posit a generating particle - the Masson (pronounced as one does the Muon). Associated with it, there is a generating function whose zeros are the masses of the particles. These masses can be projected onto a 2D Riemann Sphere of radius equal to the mass of the Masson that is determined by imposing the equivalent of a minimum action criterion; throughout this study whenever we refer to mass the intention is to the *inertial mass*.

The only particle we understand is the photon with zero mass. Ignoring other hypothetical low mass particles such as the axion or graviton<sup>5</sup>, the photon must move at the speed of light because there is no rest frame to measure the mass explicitly based on  $m_0/\sqrt{1-\beta^2}$ .

Thus, while we know how to determine the extreme [5], in general, we do not know the fundamentals underlying

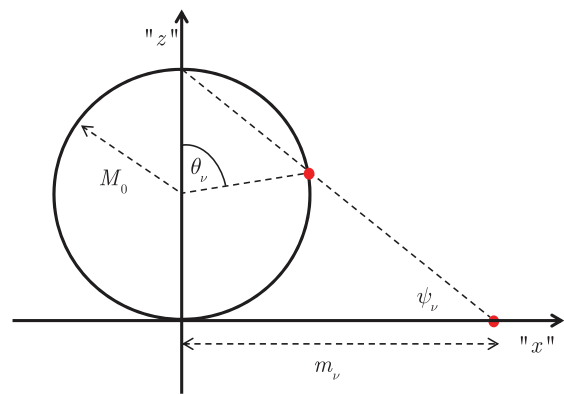


FIG. 1. The mass of a particle is marked on the axis (red-dot). Projection of the mass of the particle on the Riemann Sphere, whose radius represents the mass of the Masson  $M_0$ , is uniquely determined by the polar angle  $\theta_\nu$ .

the other values. However, we do know, according to Sommerfeld<sup>7</sup>, that it is not associated with the charge alone. He pointed out that given a macroscopic charge of finite radius and mass, the energy associated with the two is different. His approach was simple: denoting by  $E_{\text{EM}}^{(\text{rest})}$  the electrostatic energy of the charged particle when at rest and subtracting this energy from the electric and magnetic energy when the particle is in motion  $E_{\text{EM}}^{(\text{motion})}$ , it was shown that the difference does not equal the kinetic energy of the particle. Recently, the Standard Model was used to calculate the masses of 10 light hadrons as reported by Dürr et.al..<sup>8</sup> Normalizing to the mass of the  $\Xi$  baryon, they found good agreement with the observed data. Also, the mass spectrum of some 14 isoscalar tensor mesons, the so called  $f_2$  states, with masses less than 2.5 GeV have been studied.<sup>9</sup>

In this study we introduce a geometric (polar  $\theta_\nu$ ) representation of the ( $N = 279$ ) masses of the particles by employing a Riemann Sphere. This allows us to interpret

the  $N$  masses in terms of a single particle, the Masson that may be in one of the  $N$  eigen-states and whose mass we take as the radius of the Riemann Sphere as shown in Figure 1. Ignoring the other properties of these particles, it is shown that the eigen-values satisfy the symmetry  $\theta_\nu + \theta_{N+1-\nu} = \pi$  within less than 1% relative error. These eigen-values form at least 6 clusters suggestive of a “Periodic” Chart of the Particles.

## II. RIEMANN’S SPHERE

Because the range of the  $N$  masses spans over many orders of magnitude, we introduced a compact representation based on a “Riemann Sphere” as shown in Figure 1. The masses are organized in ascending order along the horizontal axis “ $x$ ”. A circle of radius  $M_0$  has its center at “ $x$ ” = 0, “ $z$ ” =  $M_0$  and the intersection of the straight-line, connecting the top of the circle with “ $z$ ” = 0, “ $x$ ” =  $m_\nu$  defines an angle  $\theta_\nu$ . Based on elementary trigonometric arguments one then finds

$$\theta_\nu = 2 \arctan \left( \frac{2M_0}{m_\nu} \right). \quad (1)$$

This transformation represents the projection of any one of the masses on the circle whose radius we attribute to the mass of the Masson. The latter is established next based on the experimental data and a minimal action criterion. To establish  $M_0$ , the vector  $\theta_\nu$  is organized in ascending order and we define the interval-spread of any two adjacent angles as

$$\mathcal{E}(M_0) = \frac{1}{\pi} \sqrt{\frac{1}{N+1} \sum_{\nu=0}^N (\theta_{\nu+1} - \theta_\nu)^2}. \quad (2)$$

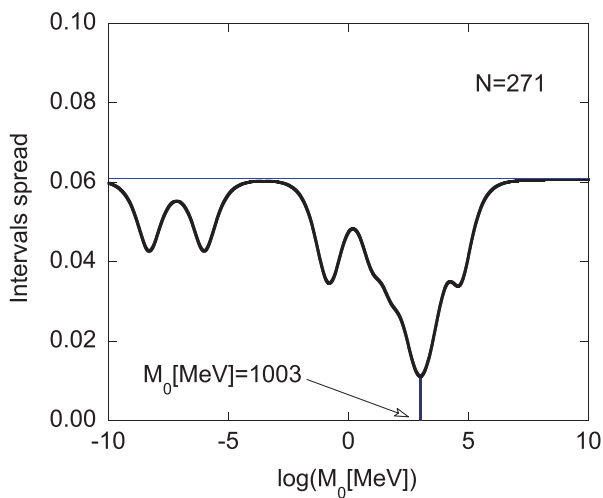


FIG. 2. Spread of intervals for  $N=279$  fundamental particles as a function of  $M_0$ . The dominant minimum is calculated numerically and it occurs at  $M_0[\text{MeV}] = 1003$  near the lowest lying baryon mass which is the only stable hadron mass.

$M_0$  is the value that *minimizes* this functional;  $\theta_{\nu=0} = 0$  and  $\theta_{\nu=N+1} = \pi$  represent the upper and lower limits of the masses in this polar representation. For the case of a *single* particle represented by an angle  $\theta$ , there are two intervals:  $\theta - 0$  and  $\pi - \theta$  so the intervals spread is proportional to  $\theta^2 + (\pi - \theta)^2$  and it has a minimum at  $\theta = \pi/2$  implying for this simple case, the radius of the sphere is half the mass of the particle i.e.  $M_0 = m/2$  or, equivalently, the particle’s mass is twice the mass of the Masson:  $m = 2M_0$ .

Now we are in position to introduce the particles from the Table in Ref. 4. The spread of their intervals in Figure 2 clearly shows resonant behavior. The absolute minimum, occurring at 1003 MeV, we take to be the mass of the Masson. For this value ( $M_0 = 1003$  MeV) the Riemann Sphere is illustrated in Figure 3. Two facts are evident – first, as anticipated, most of the particles are located in the  $\theta \sim \pi/2$  region and, second, close to zero and  $\pi$  there are voids with no particles although these are not symmetrically disposed nor do they appear to be correlated in any obvious way but more on this later.

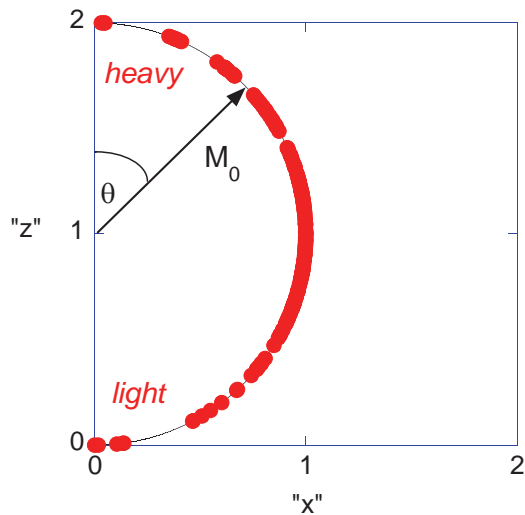


FIG. 3. Projection of the masses of all 279 particles where the mass of the Masson is determined from the requirement that the spread of the intervals in Figure 2 is minimal. Light particles ( $\theta \sim \pi$ ) are the gamma, gluon and neutrinos. The heavy ones ( $\theta \sim 0$ ) the gauge-particles, Higgs and top quark.

## III. CHARACTERISTICS OF THE POLAR REPRESENTATION

With the polar representation established, we now investigate some features of the inertial masses based on this new representation. To begin, consider only the hadrons ( $N = 261$ ). If we were to establish the Masson based on the hadrons alone, its mass would be only slightly reduced to  $M_0^{(H)} = 962.2$  MeV. Moreover, if we attribute a separate Masson to baryons ( $N = 113$ ) and to mesons ( $N = 148$ ) the corresponding Masson masses

would be  $M_0^{(B)} = 1094$  MeV and  $M_0^{(M)} = 964$  MeV. All of these and esp.  $M_0^{(H)}$  and  $M_0^{(M)}$  are close to both  $M_0$  as well as to the stable nucleon mass  $N(940)$ . Curiously, there are more mesons than baryons even though their confined quarks(2) are fewer than for the baryons(3). In all cases, the corresponding “intervals spread”, similar to Figure 2 for all of the particles, gave a *single* minimum.

Another perspective on the polar representation of the masses can be obtained by ordering the  $\{\theta_\nu\}$  in ascending order and plotting them as a function of the normalized index  $\nu$  (quantum number) as the red squares in Figure 4. For comparison, the  $N$  zeros of the Legendre polynomial of order  $N = 279$  are organized in ascending order and represented by the black squares  $[P_N(\cos \zeta_\nu) = 0; \nu = 1, 2, \dots, N]$ . While the latter is virtually linear, the former has a more complex structure with distinct “band-gaps” in the range  $\nu < 0.2N$  and  $\nu > 0.9N$ .

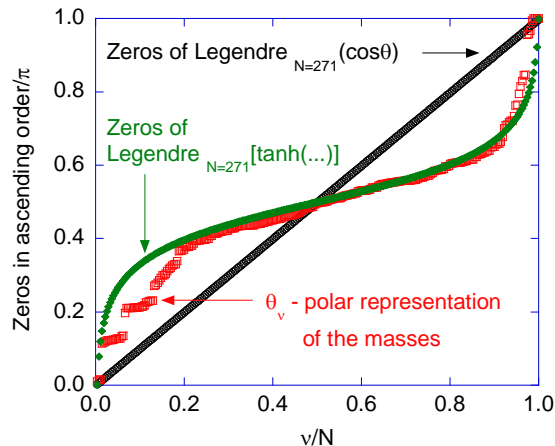


FIG. 4. Red squares represent the masses ( $\theta_\nu$ ) in ascending order and the black squares the zeros of the Legendre function of order  $N = 279$ . The green diamonds are discussed in the text below. The index  $\nu$  is normalized by  $N$ .

Two observations may be made: (i) if the absolute value of the argument of the Legendre polynomial is larger than unity the behavior is hyperbolic and the function has no zeros in this range. This is consistent with the existence of band-gaps. (ii) Having in mind that the argument of the Legendre polynomial ( $\cos \theta$ ) varies between  $-1$  and  $1$ , we consider another function which is defined in this range ( $\tanh$ ) and we calculate the zeros of  $P_N \left[ \tanh \left( 3.46 \left( \pi/2 - \theta_\nu^{(M)} \right) \right) \right] = 0$  which are represented by the green squares in Figure 4. In the range  $0.2 < \nu/N < 0.9$  these zeros approximate the polar representation of the masses ( $\theta$ ) with an accuracy of 0.07% being defined as  $100 \times \left\langle [1 - \theta_\nu^{(M)}/\theta_\nu]^2 \right\rangle_\nu$ . What these results indicate is that the  $\theta_\nu$  might be regarded as the eigen-values of a characteristic polynomial of the Legendre type. Our approach in this was inspired by the work of Liboff and Wong<sup>10</sup> in connection with their study of

the prime numbers and the zeta function.

Having such a representation in mind, an additional feature is revealed by examining the sum of the eigen-values. Let us assume that we know the Hamiltonian whose eigen-values are  $\theta_\nu^s$  wherein  $s$  is a free parameter to be determined. In many cases of interest, the measurable is given by a term of the form  $\text{Trace}(H)$  which in turn is proportional to  $g(s) \equiv \sum_\nu \theta_\nu^s$ . In reality we do not know this Hamiltonian but a rough idea as to its character can be obtained by assuming that  $g(s)$  has a minimum. A simple calculation reveals that such a minimum exists for  $s \simeq -79/150 = -0.5267$ .

One of the main results of our approach relies on a property of the Legendre polynomials that the sum of *two zeros* of complementary order ( $\nu + \nu' = N + 1$ ) equals  $\pi$ , or explicitly  $\zeta_\nu + \zeta_{N+1-\nu} = \pi$ . We have examined to what extent this rule applies to the polar representation of the masses ( $\theta_\nu$ ) and found that  $\theta_\nu + \theta_{N+1-\nu} = \pi\chi$  with  $\chi = 0.958$  within 0.13% relative error defined as

$$\text{Error}[\%] = 100 \frac{1}{2N} \sum_{\nu=1}^N \left[ \frac{\theta_\nu + \theta_{N+1-\nu} - \pi\chi}{\theta_\nu + \theta_{N+1-\nu}} \right]^2. \quad (3)$$

The factor of 2 in Eq.(3) corrects the fact that each pair of masses is counted twice. According to the present spectrum of masses [4], this relation implies that the mass of the Higgs and that of the Axion (if observed) would be related  $\theta_{\text{Axion}} + \theta_{\text{Higgs}} \simeq \pi$  and that the mass of the electrons neutrino is related to that of the Z-gauge boson  $\theta_{\nu_e} + \theta_Z \simeq \pi$  [5]. However, it should be emphasized that the present estimate of the error is dominated by the light particles with  $\theta \sim \pi$  and that it is larger if the deviation is compared to the smallest angle between the two. In fact, due to uncertainty associated with the measurement of many of those masses and especially the neutrinos, comparing to the calculated deviation of  $\chi$  from unity, one can hypothesize that  $\chi \equiv 1$  or explicitly

$$\theta_\nu + \theta_{N+1-\nu} = \pi. \quad (4)$$

For further insight into this result, we plot in Figure 5 the normalized symmetry-pairs  $(\theta_\nu + \theta_{N+1-\nu})/\pi$  as a function of the normalized masses  $(\theta_\nu/\pi)$ . Several important aspects are reflected in this plot: (i) the pairs linked by Eq.(4) form (at least) six clusters although a better picture will be shown later. (ii) The error or deviation from unity is dominated by light particles ( $\theta \sim \pi$ ). When both particles have similar mass, the deviation is negligible – see the right cluster. (iii) Further splitting is expected when including additional quantum numbers that produce a Riemann hypersphere. (iv) Subject to the condition  $\chi \equiv 1$ , the error defined above for hadrons is 0.47%, for baryons 0.07% and for mesons it is 0.63%.

Before proceeding it is important to assess whether such small errors are not the result of pure coincidence. For this purpose let us postulate that the Masson has a fixed inertial mass of  $M_0 = 1003$  MeV and between the

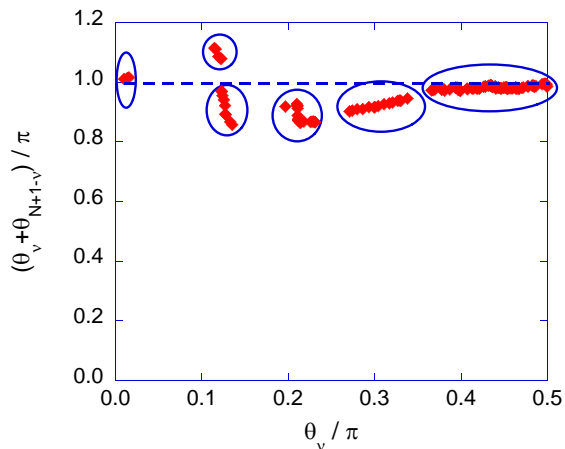


FIG. 5. The normalized symmetry-pairs,  $(\theta_\nu + \theta_{N+1-\nu})/\pi$ , as a function of the normalized geometric representation of the masses  $(\theta_\nu/\pi)$ . These pairs form at least six clusters analogous to a “Periodic Table” for the fundamental particles.

two extremes, the photon and the top quark, the various (279) particles are randomly distributed. We represent the inertial masses in terms of a random variable  $m_\nu [\text{MeV}] = 10^{p_\nu}$  wherein  $p_\nu$  is uniformly distributed  $-8 \leq p_\nu \leq 5 + \log(1.26) = 5.104$ . As in the case of the real particles, we employ the transformation in Eq. 1. It is tacitly assumed that the mass of the Masson is not dependent on the specific distribution. Once the  $\theta_\nu$  are established, the error is calculated based on Eq. 3. We determined this error 1000 times, each time for a different seed. The resulting error spans from 7% to less than 11%. Figure 6 shows the error as a function of the index of the seed ( $1 \leq n \leq 1000$ ). For comparison, in the case of all of the actual particles (279), its value is 0.225% indicating that the roughly two orders of magnitude difference is not a result of coincidence.

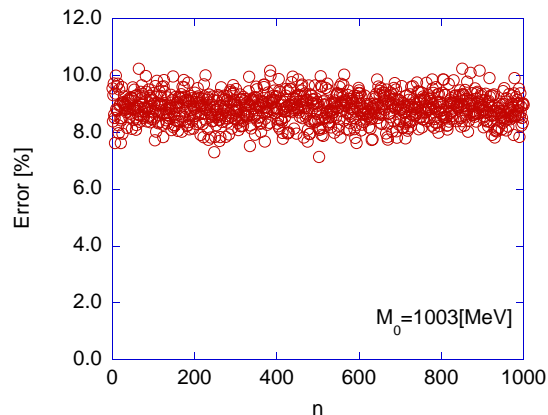


FIG. 6. The error associated with the polar representation of a random distribution of masses for 1000 different seeds. The value for the actual particles is 0.225%.

#### IV. SOME FUNDAMENTALS

Hadrons are the absolute majority (261) of the 279 fundamental particles we have considered and we have called them fundamental because they are composite being made of different numbers of quarks, gluons and antiquarks as opposed to those one might call elementary such as the electron. These particles can also be distinguished as bosons or fermions according to their individual spins. The elementary fermions include two classes – the quarks and leptons whereas the elementary bosons comprise the photon and gluons. We have *not* included any antiparticles in our particle count because they bring nothing new to our analysis and because, as far as we know, there has never been a fermion discovered that did not lead to the discovery of its corresponding antiparticle as first implicitly suggested by Dirac.<sup>11</sup>

#### V. BARYONS AND MESONS

We now take a closer look at the mesons (148) and baryons (113) separately and compare the two species. The Masson is assumed to have a fixed mass as determined above ( $M_0 \equiv M_{\text{Masson}}$ ) and in the first row of Figure 7 we plot the polar intervals spread for both mesons and baryons - similar to the process that lead to Figure 2 except these spreads are only for mesons or baryons separately. A good approximation to the exact expression in Eq. (2), the (red) solid-line, is given by a simple Lorentzian (black) dashed-line corresponding to a band-pass model

$$\mathcal{E}_{\text{model}}(M) = \mathcal{E}_{\text{max}} + \frac{\mathcal{E}_{\text{min}} - \mathcal{E}_{\text{max}}}{\sqrt{1 + Q^2 \left( \frac{M}{M_{\text{Masson}}} - \frac{M_{\text{Masson}}}{M} \right)^2}}$$

The spread of meson masses ( $\Delta M = 5447 [\text{MeV}]$ ) is more than twice the spread for the baryons ( $\Delta M = 2506 [\text{MeV}]$ ). Note that in these two cases, the intervals spread has a *single* resonance in direct contrast to the picture in Figure 2 for all of the particles.

The central frames in Figure 7 show the normalized density of states (DoS) projected on a Riemann sphere when the arc is divided into 60 segments and a cubic spline is used to approximate the DoS function. Two comments may be made: (i) The resonance character of the DoS is clearly revealed and (ii) the voids and structure in the DoS are more pronounced for the mesons. The bottom frames illustrate the complementary symmetry for each species. For the mesons we see 5 sub-groups but only 3 for the baryons but both types of particle show a rough mirror symmetry about  $\theta \simeq \pi/2$ .

#### VI. SPIN

At this point we introduce information about the total spin  $J$ . The four frames of Figure 8 reveal the polar rep-

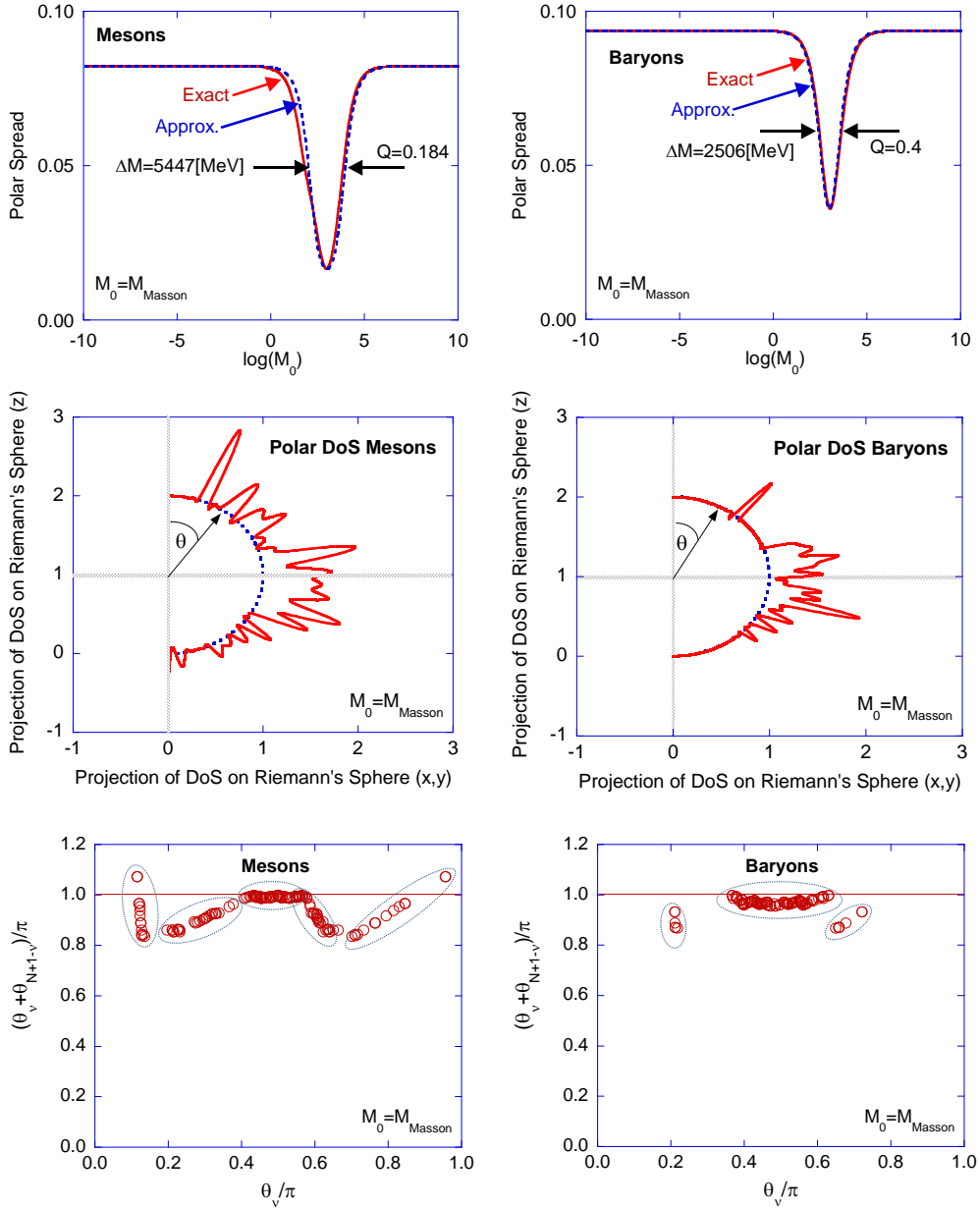


FIG. 7. Mesons (148) left-column and baryons (113) right-column are considered separately. The Masson is assumed to have the mass as determined above  $M_0 = M_{\text{Masson}}$  and in the first row the polar intervals spread for both mesons and baryons are shown - similar to the process that lead to Figure 2 except the spread is only for mesons or baryons independently. A good approximation to the exact expression [Eq. 2], (red) solid-line, is given by a simple Lorentzian (black) dashed-line corresponding to a band-pass model. Central frames reveal the normalized density of states (DoS) projected on a Riemann sphere; the arc was divided into 60 segments and a cubic spline was used to approximate the DoS. Two comments are: (i) The resonance character of the DoS is clearly evident and (ii) the voids in the DoS are more pronounced for the mesons. Bottom frames illustrate the complementary symmetry for the mesons and baryons. For the mesons we identify 5 sub-groups but only 3 for the baryons.

resentation of the masses as a function of the quantum number ( $\nu$ ) wherein the red circles represent the bosons (integer spins) and the blue crosses show the fermions (non-integer). The top-left frame reveals the full range whereas the other frames are a breakdown or magnification of the full range into three parts. Two facts are evident from the top-left frame: (i) there are obvious

voids at both low and high energy ends, (ii) bosons occupy most of the low-energy states ( $\theta \sim \pi$ ) i.e. most of the lower-right frame.

At high energies (top-right frame) the voids become more distinct and there is no indication of a preferred species (fermion or boson) in any one of the “energy-bands” with the exception of the last one at  $\nu/N \sim 0.2$ .



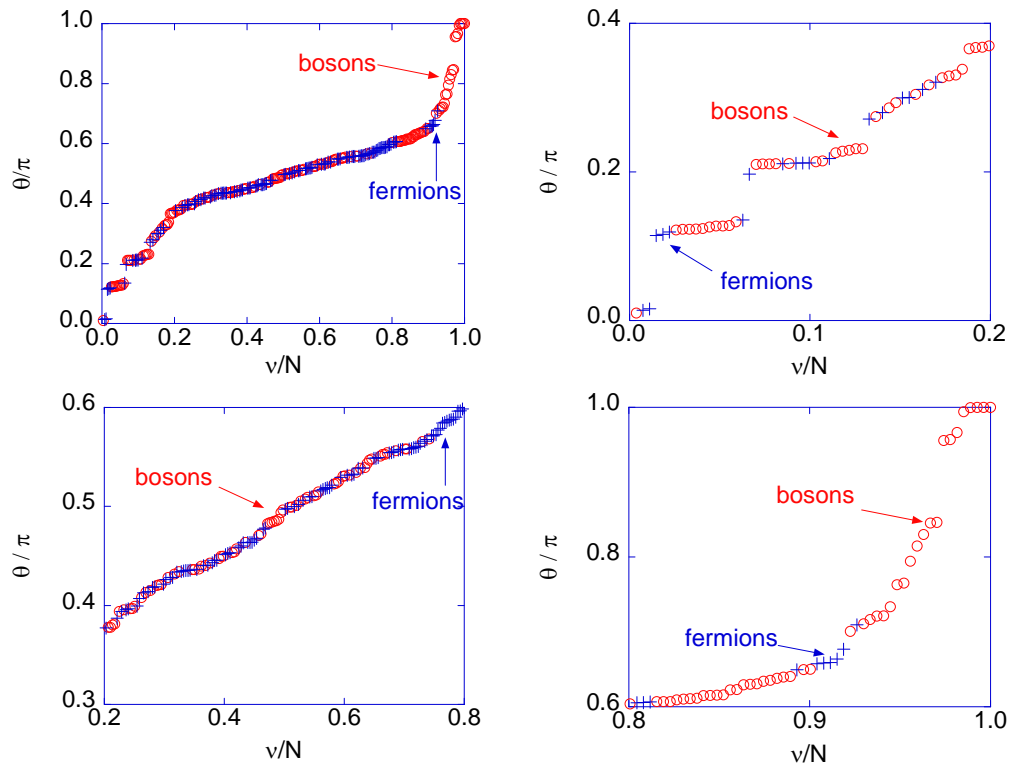


FIG. 8. Polar representation of the masses vs the quantum numbers for fermions(blue crosses) and bosons(red circles).

In the central energy range ( $0.2N < \nu < 0.8N$ ), bottom-left frame,  $\theta$  is almost linear in  $\nu$  and at the adopted resolution, there are, at most, two voids: (i) close to  $\theta \sim \pi/2$  there is an interval that is fermions-free and (ii) at the top end there is a region that is bosons-free. With higher resolution, additional voids can be identified. Over the central range one sees a slight third order variation that gets magnified at the wings e.g. in the lower right frame. Finally, at the low energy end (bottom-right frame), bosons dominate with four or five voids that are boson-free. Without more quantum numbers, we have no explanation for this “band-gap” structure other than greater sensitivity to the underlying quark masses and dynamics analogous to the periodic table of the elements whose structure is now understood to be determined by the effects of the Pauli exclusion principle in atomic physics.

Another observation refers to the distribution of fermions and bosons between spin-states. Figure 9 shows these distributions when each is normalized to unit area. Several comments can be made: (i) the peak distribution for the fermions is at the lowest state ( $J = 1/2$ ) whereas the distribution of the bosons peaks at the first “excited state” ( $J = 1$ ) and not the “ground state”. Note that we have used  $J$  and  $S$  interchangeably for the total spin. (ii) The average quantum-number for bosons is close to  $\langle J \rangle \sim 1$  while for fermions it is  $\langle J \rangle \sim 1.5$ . This contradicts distributions of single species of either bosons or fermions where in thermodynamic equilibrium, the highest likelihood is always the lowest energy or “ground

state” and this is also consistent with a spin-independent Hamiltonian formulation. (iii) For both species, the spread is similar.

Figure 10 shows the spin  $J$ ,  $\theta$  and the symmetry  $\theta_\nu + \theta_{N+1-\nu}$ . Clearly, there are two major voids: the one on the left indicates no particles with spin larger than  $1 + \theta^3$  and, on the right, that there are no lighter particles having  $\theta > 0.6\pi$  with a spin larger than 2. Explanations for these voids follow from our expectation that the highest spins should lie near the highest density of states i.e. towards the middle around  $\theta \sim \pi/2$  i.e. away from the endpoints at 0 and  $\pi$  and that such states do not occur in isolation but as members of spin multiplets.

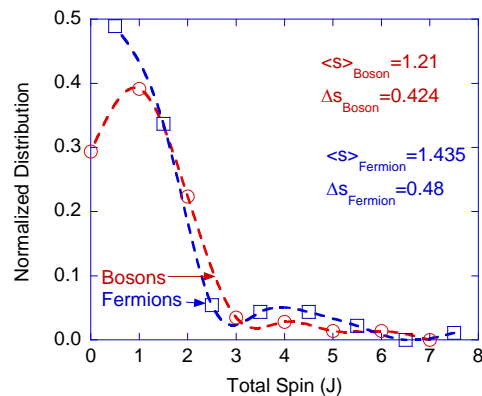


FIG. 9. Comparison of spin distributions: fermions(blue) and bosons(red). Fermions peak at one-half and bosons at one.

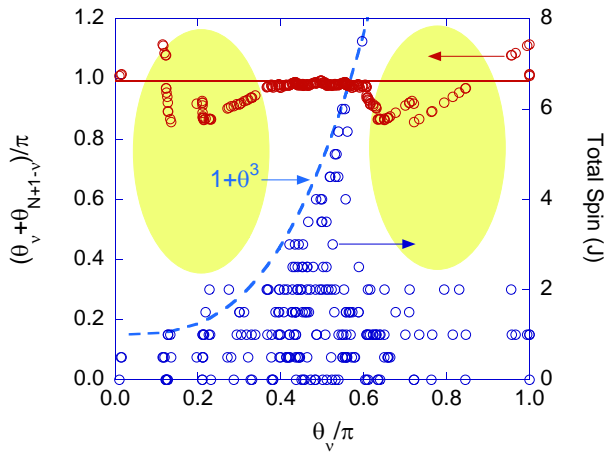


FIG. 10. The total spin  $J$ ,  $\theta$  and the symmetry  $\theta_\nu + \theta_{N+1-\nu}$  are shown with two major voids (colored). The one on the left indicates that there are very few particles with a spin larger than  $1 + \theta^3$  and, the one on the right, that there are no lighter particles having  $\theta > 0.6\pi$  with a spin larger than 2.

## VII. CONCLUSIONS

A geometric representation of the  $N = 279$  **inertial masses** of the elementary and lowest lying fundamental particles was introduced by employing a Riemann Sphere. It allowed us to interpret the  $N$  masses in terms of a single entity, the Masson, that might be in one of the  $N$  eigen-states. Geometrically, the mass of the Masson was the radius of the Riemann Sphere while its numerical value was closest to the mass of the nucleon regardless of whether  $M_0$  was computed from all particles (279), the hadrons (261), or just the mesons (148) or baryons (113).

Ignoring the other properties of these particles, it was shown that the eigen-values, the polar representation  $\theta_\nu$ , satisfied a symmetry  $\theta_\nu + \theta_{N+1-\nu} = \pi$  within less than 1% relative error. One thousand samples consisting of 279 masses chosen randomly over the observed mass range

gave much larger errors e.g. none were less than a factor of 30 larger. A function was established whose zeros were, to good approximation, the polar representation of the masses  $\theta_\nu$ . A rough assessment of the Hamiltonians' character was made by imposing that its trace  $\sum_\nu \theta_\nu^s$  has a minimum for  $s = -0.523$ .

Among other results we found that bosons occupy most of the light mass states and there are virtually no fundamental particles with spin  $J$  larger than  $1 + \theta^3$ . Among hadrons we found that mesons form 5 clusters whereas baryons form 3 but both groups have a similar structure being roughly symmetric about  $\theta_\nu = \pi/2$ .

The new symmetry and its extension pairing bosons and fermions based on grouping all of the degenerate zero mass particles into one we called the "photon" holds well for the gauge bosons and lowest lying leptons and quarks until one has to pair hadrons because the quarks and leptons are fermions while the highest lying hadrons are bosons based on high lying, quark-antiquark mesons.

We did not include antiparticles in our analysis based on quantum field theory where every fermion has a corresponding antifermion of identical mass<sup>11</sup> because they added nothing new. Nevertheless, they are important for cosmology where the lack of any apparent antimatter in the universe is a concern albeit ironic<sup>12</sup>. Because the only stable hadron is the relatively heavy nucleon presumably because it contains no antiquarks one sees the weakness of using only classical concepts in an attempt to understand the microscopic particle world.

## ACKNOWLEDGMENTS

We acknowledge one of the great scientific achievements on this approximate anniversary of Mendeleev's Periodic Table of the Elements. Also, we especially wish to thank Stan Brodsky, Achim Weidemann and Kent Wooton for their comments and help with the manuscript. This work was supported in part by Department of Energy contract DE-AC02-76SF00515.

<sup>1</sup> Edwin Arthur Burtt, *The Metaphysical Foundations of Modern Physical Science*, (Routledge and Keegan Paul LTD, London, Revised Edition, 1932).

<sup>2</sup> Albert Einstein, "Elementary Derivation of the Equivalence of Mass and Energy," in *The Eleventh Josiah Willard Gibbs Lecture*, (Pittsburgh, 1934). Albert Einstein, "Ist die Trägheit eines Körpers von seinem Energiegehalt abhängig?," *Ann. Der Physik* **17**, (1905).

<sup>3</sup> We take as given that the equations of motion represent a set of coupled equations including all relevant variables with their couplings explicit e.g. the spins and isospins and whether we are solving the Lorentz equations, the Klein Gordon, the Dirac or the QCD Lagrangian, the mass of a particle or its reduced Compton wavelength always appears explicitly e.g. as a baseline potential.

<sup>4</sup> *Rev. Part. Prop., Phys. Lett. B*, Vol. **667/1** (1-1340)

(2008). Also: *Rev. Part. Phys., J. Phys. G*, Vol. **37**, 7A(1-1422) (2010). The exact Table used can be found at <http://webee.technion.ac.il/people/schachter/AppendixMassesofFundamentalParticles.pdf>

<sup>5</sup> We take the "rest mass" as simply "mass" – a relativistic invariant with neither "rest" nor the subscript "0" attached except for our hypothetical Masson  $M_0$ . The *observed* masses [4] are understood to be somewhat greater than the bare mass due to self interaction contributions. The Axion was included in the Table but not used and because we did not consider gravity, the graviton was not included. Neither of these have yet been observed.

<sup>6</sup> Because the error bars on the neutrino masses are large, we assume their masses are all much lighter than the electron's based on the standard model of cosmology.

<sup>7</sup> Sommerfeld A. , *Electrodynamics in Lectures on Theoretic-*

- cal Physics*, (Academic Press, New York, 1952), pp. 278.
- <sup>8</sup> S. Dürr, Z. Fodor, J. Frison, C. Hoelbling, R. Hoffmann, S. D. Katz, S. Krieg, T. Kurth, L. Lellouch, T. Lippert, K. K. Szabo, and G. Vulvert, "Ab Initio Determination of Light Hadron Masses," *Science*, **322**, 1224 (2008).
- <sup>9</sup> Zao-Chen Ye, Xiao Wang, Xiang Liu and Qiang Zhao, "The mass spectrum and strong decays of isoscalar tensor mesons", arXiv.org, hep-ph, arXiv:1206.0097v2 (2012).
- <sup>10</sup> Richard L. Liboff and Michael Wong, "Quasi-Chaotic Property of Prime-Number Sequence", *Int. J. Theo. Phys.* **37**, 3109-3117 (1998).
- <sup>11</sup> P. A. M. Dirac, "The Quantum Theory of the Electron", *Proc. Roy. Soc. A: Math., Phys. & Eng. Sci.* **117**, 610 (1928).
- <sup>12</sup> Large (1 km across) isolated clouds of positrons may have been observed recently but with short lifetimes (0.2 s) – see J.R.Dwyer et al., *J. Plasma Physics* **81**, 475810405 (2015).